

collisions is too small to be observed with our experimental accuracy. We find that $\gamma = \tau_2/\beta = 4.1 \pm 0.3$ nsec Torr, which agrees well with the result of Ref. 2. Here we have used τ_2 , because the collisions give no effect on the decay of the echo between the second and the third pulse.

At this point we want to make a remark about the relationship between our backward three-pulse echo and the trilevel echo by Mossberg *et al.*⁷ The former may be considered as a two-level version of the latter in the sense that the third and ground levels are degenerate.

We have discussed the general case of three-pulse echoes on two-level systems in solids and gases. One example of the backward echoes has been demonstrated on the Na D line with a simple experimental setup. In this study, it is shown that in Na-Ar collisions the velocity-changing collisions are negligible compared with the phase-interrupting ones. Finally, we point out several advantages of backward echoes: (i) easy elimination of excitation pulses, (ii) applicability to the

picosecond regime, and (iii) wide range of applicability to the problems of two-level systems from solids to gases.

¹N. A. Kurnit, I. D. Abella, and S. R. Hartmann, Phys. Rev. Lett. **13**, 567 (1964); I. D. Abella, N. A. Kurnit, and S. R. Hartmann, Phys. Rev. **141**, 391 (1966).

²A. Flusberg, T. Mossberg, and S. R. Hartmann, Opt. Commun. **24**, 207 (1978).

³T. Baer and I. D. Abella, Phys. Rev. A **16**, 2093 (1977).

⁴R. G. Brewer and R. L. Shoemaker, Phys. Rev. Lett. **27**, 631 (1971); R. G. Brewer and A. Z. Genack, Phys. Rev. Lett. **36**, 959 (1976).

⁵M. Scully, M. J. Stephen, and D. C. Burnham, Phys. Rev. **171**, 213 (1968).

⁶N. S. Shiren, Appl. Phys. Lett. **33**, 299 (1978). He discussed Fig. 1(c) of the [A] term, and concluded that the backward echo could not be formed in a gas.

⁷T. Mossberg, A. Flusberg, R. Kachru, and S. R. Hartmann, Phys. Rev. Lett. **39**, 1523 (1977).

High-Power, cw, Efficient, Tunable (uv through ir) Free-Electron Laser Using Low-Energy Electron Beams

Luis R. Elias

Department of Physics and High Energy Physics Laboratory, Stanford University, Stanford, California 94305
(Received 16 January 1979)

Using beams of low-energy electrons ($E < 5$ MeV), a free-electron laser can be operated as a continuously tunable ($1000 \text{ \AA} < \lambda < 50 \text{ \mu m}$), high-power ($P > 10$ kW, cw) source of laser radiation. With electrostatic accelerators the electron beam can be recycled to increase the overall efficiency of the laser. Wall power to laser power efficiencies greater than 10% are possible.

The amplification of optical radiation by a beam of relativistic electrons moving through a static, spatially periodic transverse magnetic field, proposed by Madey in 1971,¹ was demonstrated by Elias *et al.*² In 1977 Deacon *et al.*³ reported the operation of the free-electron laser (FEL), above threshold, as an optical oscillator at a wavelength of 3.4 μm .

Lasers based on the technique used in these Stanford experiments are important because they have the potential capability of operating as sources of optical radiation with the following highly desirable characteristics⁴: (a) high average output power, (b) broadband continuous wavelength tunability, (c) high optical resolution, and (d) very high overall efficiency.

The prospect for high-power operation stems from the experimental result³ that nearly 0.2% of the electron kinetic energy can be converted to optical radiation. Characteristic (b) arises, principally, from the dependence of wavelength on electron energy. The range of energies available from present electron accelerators is quite large. Laser operation can thus be obtained at wavelengths anywhere between 1 mm and 1000 \AA . Characteristic (c) stems from the observed ability of the FEL to radiate a homogeneously broadened spontaneous spectrum.

The capability (d) of operating the FEL at high overall efficiency has received considerable recent attention. As was noted earlier, in the Stanford experiments, a maximum of 0.2% of the elec-

tron kinetic energy is converted to optical radiation. The rest of the electron energy (99.8%) is wasted.

It has long been suggested that to improve efficiency and power in a FEL the electron beam should be recirculated.⁴ To that effect, various groups⁵ are presently studying the operation of the FEL in an electron storage ring. As a result, several schemes have been formulated to obtain efficient FEL operations with rf accelerators; however, the feasibility and cost of their concepts still remain to be determined.

Electrostatic accelerators produce electron beams of very high quality and can be used with periodic magnetic structures to produce laser oscillations in the far-infrared region ($\lambda > 13 \mu\text{m}$). To increase efficiency⁶ the output electron beam can be collected at high negative potential (low kinetic energy) when a second electrostatic decelerator is used. The amount of energy lost by the electrons to laser radiation on a steady-state basis can be given back to the electrons from a relatively low-voltage dc emf generator. Although, the prospects for efficient FEL operation by this method is excellent, the technique has not received proper attention because of the restricted range of wavelengths ($\lambda \approx \lambda_q/2\gamma^2 \geq 13 \mu\text{m}$) at which the FEL can operate using low-energy ($E = \gamma mc^2 \leq 10 \text{ MeV}$) electron beams with static magnetic structures ($\lambda_q > 1 \text{ cm}$).

This Letter describes a novel technique in which the static magnetic structure of a conventional FEL is replaced by an equivalent intense TEM pump wave whose period (λ_p) can be made arbitrarily short. When low-energy recirculating electron beams are used, the technique offers the possibility of efficient, high-power, tunable [$1000 \text{ \AA} < (\lambda \approx \lambda_p/4\gamma^2) < 50 \mu\text{m}$] FEL operation.

In the single-particle classical description of a free-electron laser⁷ an input TEM wave can be amplified by extracting energy, via the Lorentz force equations, from an electron moving along the direction of propagation of the wave. To accomplish this, the electron must, initially, be given a transverse velocity modulation of the proper periodicity and phase. A periodic magnetic structure, such as the one used in the Stanford experiments, provides the means to periodically accelerate the electrons in the transverse direction. This technique has the following ideal features: (a) the velocity modulation is done with little expenditure of energy when permanent or superconducting magnets are used, (b) the magnetic field strength required to operate the laser

above threshold ($B > 0.1 \text{ T}$) can be readily obtained, and (c) for high-power cw operation the magnetic field is present on a continuous basis (i.e., the field is static).

A real pump wave with approximately the same characteristics as the ones described above can be produced in a conventional free-electron laser operating inside a far-ir low-loss optical cavity. The optical power density required for operation above threshold falls in the range of $S = 10^8 - 10^9 \text{ W/cm}^2$. To eliminate detrimental electron-beam charge-density effects⁸ the cross section of both the pump wave beam and electron beam should be larger than 1 cm^2 when tens of amperes of electron beam current are used. The minimum total optical-pump-wave power inside the cavity is thus $10^8 - 10^9 \text{ W}$ (cw). Other authors have discussed the possibility of using ir lasers⁹ and microwave sources¹⁰ as pump-wave sources. However, present lasers fail to meet simultaneously the pump-wave requirements [(a), (b), and (c)] discussed above. High-Q microwave cavities, on the other hand, can fulfill these requirements. However, microwave wavelengths are too long to be used with low-energy electron beams to produce visible laser radiation. The ideal pump wavelength region is the far ir.

Strong interaction occurs between the pump wave, the input wave, and the electron beam (see Fig. 1) when

$$\gamma_R^2 = \frac{(\lambda_p + \lambda)^2}{4\lambda_p\lambda} \left[1 + \left(\frac{e\lambda_p B_p}{2\pi mc} \right)^2 + (\gamma\theta)^2 \right], \quad (1)$$

where B_p is the rms value of the pump-wave magnetic field and θ is the angle between the electron's drift velocity and the direction of the pump wave. Attenuation of the input wave occurs when $\gamma \lesssim \gamma_R$. Using the Lorentz force equations it can be shown that the average amount of energy gained by the electron during the wave-amplification process is given by

$$\langle \delta\gamma \rangle = \frac{1}{2\pi} \int_{\theta=0}^{2\pi} \int_{t=0}^{t=\tau} \frac{e\vec{E} \cdot \vec{V}}{mc^2} dt d\theta, \quad (2)$$

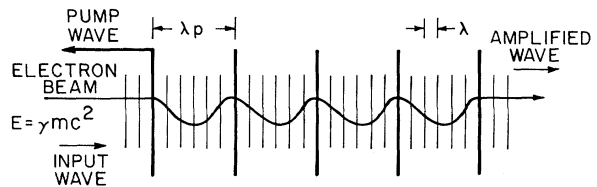


FIG. 1. Simple laser interaction geometry including pump wave, input wave, and electron beam.

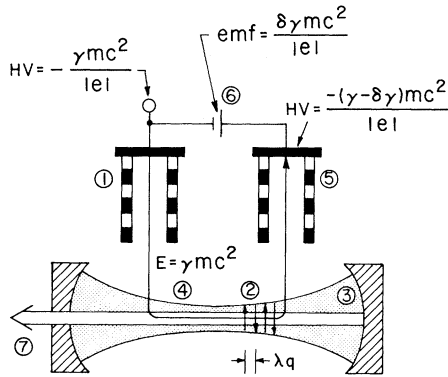


FIG. 2. A simple scheme using a single beam of low-energy recirculating electrons.

where \vec{E} is the electric field of the input wave, \vec{V} is the electron velocity vector, θ is the initial optical phase of the electron's transverse motion, and τ is the interaction time.

Figure 2 schematically illustrates a complete FEL configuration using the new technique. A continuous beam of monochromatic electrons of energy $E = \gamma mc^2$, emerging from the dc accelerating column (1) interacts with the periodic magnetic structure (2) to produce laser oscillations (3) (pump wave) at a wavelength $\lambda_p \approx \lambda_q / 2\gamma^2$ in the far-ir region. For high efficiency, the losses in the far-ir cavity are kept to a minimum ($\sim 0.1\%$).

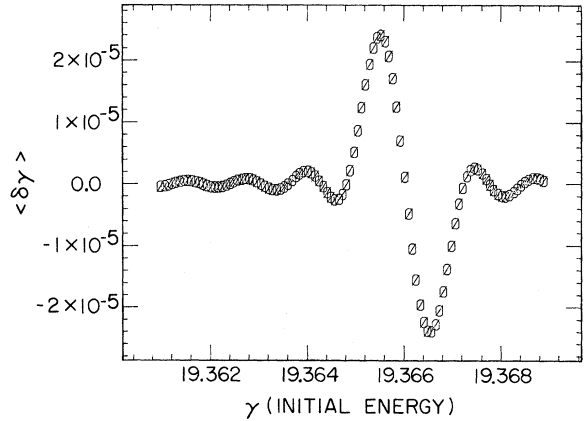


FIG. 4. Average energy $\langle \delta\gamma \rangle mc^2$ gained per electron for the short-wavelength laser illustrated in Fig. 3. The horizontal axis describes the initial energy of the electron beam. ($\lambda = 4000 \text{ \AA}$, $\lambda_p = 600 \mu\text{m}$, $B_p = 0.05 \text{ T}$, interaction length = 2.4 m.)

The same electron beam interacts with the pump wave in region (4) to produce laser oscillations at a shorter wavelength $\lambda \approx \lambda_p / 4\gamma^2$. The output short-wavelength beam is shown at (7). To increase efficiency and power the output electron beam is decelerated in column (5) and collected at a high negative potential as shown. This configuration is simple but it does not provide proper optimization of the small-signal power gain at

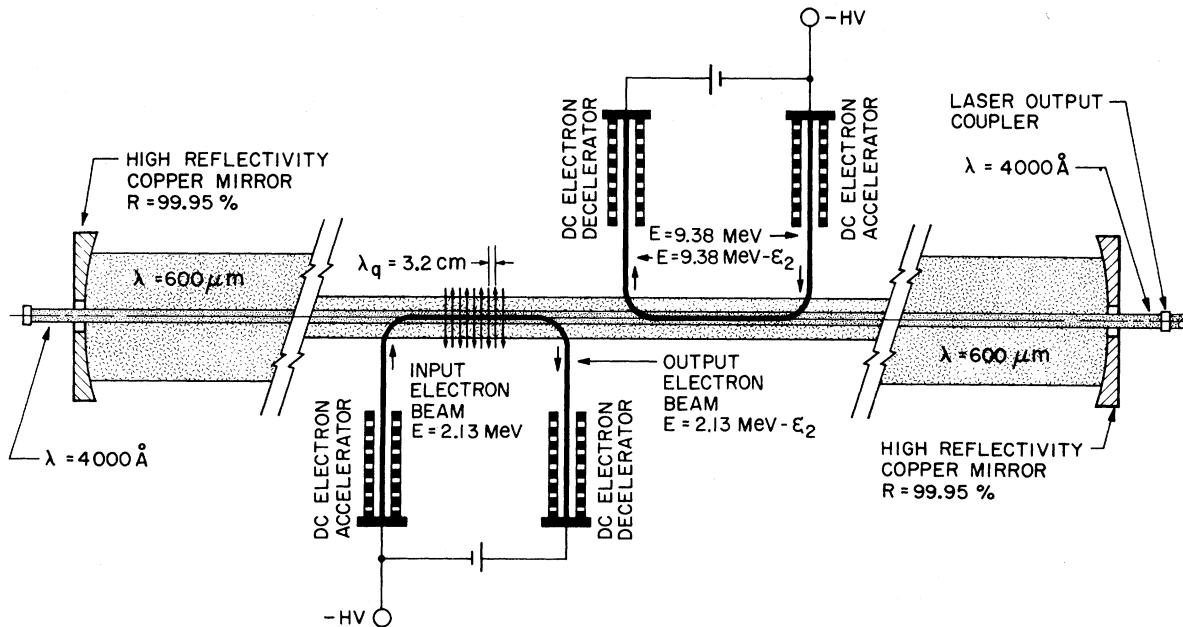


FIG. 3. A more complex scheme using two independent electron beams to optimize the small-signal gain of the short-wavelength ($\lambda = 4000 \text{ \AA}$) laser.

TABLE I. Typical laser operating characteristics and electron-beam requirements for the scheme shown in Fig. 3.

	$\lambda = 4000 \text{ \AA}$	$\lambda = 16 \text{ }\mu\text{m}$
Optical Beam		
Pump-wave power density	250 MW/cm ²	60 MW/cm ²
Pump wavelength	600 μm	4 mm
Interaction length	2.4 m	1.2 m
Small-signal gain	12.5%/pass	16%/pass
Saturated-signal gain	5%/pass	8%/pass
Power output (cw)	12.5 kW	40 kW
Efficiency	0.3%	1.5%
Electron beam		
Current	25 A	20 A
Energy	9.38 MeV	3.55 MeV
Energy homogeneity		
$\Delta\gamma/\gamma$	6×10^{-5}	0.8×10^{-3}
Maximum beam emittance	0.8 mm mrad	10 mm mrad

short wavelengths. It can be shown^{1,7,11} that the maximum small-signal gain for such a laser is given by

$$G_{\text{max}} = \text{const} \times \rho_e B_p^2 \lambda^{3/2} \lambda_p^{5/2} N^3, \quad (3)$$

where ρ_e is the electron density and N is the number of pump-wave periods in the interaction region. For fixed N , the gain varies as $\lambda_p^{5/2}$. It is clear that for optimum small-signal gain at a specified wavelength it is advantageous to use the longest possible pump wavelength subject to the additional constraint imposed by Eq. (1). Figure 3 illustrates a more complex scheme in which two independent electron beams are used to optimize the small-signal gain of the laser at $\lambda = 4000 \text{ \AA}$ using 9.38-MeV electron beams. For such a configuration, the average energy [$\Delta E = \langle \delta\gamma \rangle mc^2$] gained per electron is shown in Fig. 4. The results shown were obtained by integrating Eq. (2) numerically in the small-signal regime. The actual power gain per pass is given by $-\langle \delta\gamma \rangle mc^2 I / eSA$, where S and A are, respectively, the optical power density and mode cross section of the input wave in the interaction region.

The number of pump-wave periods N in the interaction region determines the homogeneously broadened width of the spontaneous radiation spectrum $\Delta\gamma/\gamma = 1/2N$. Solving for λ in Eq. (1), it is possible to derive restrictions⁴ on the electron beam characteristics such that no inhomogeneous spontaneous spectral broadening is introduced by the beam. The restrictions are (a) electron-energy homogeneity $\Delta\gamma/\gamma \leq 1/2N$, (b) maximum electron-beam divergence $\theta \leq (\lambda/N\lambda_p)^{1/2}$, and

(c) maximum electron-beam radius $r \leq \omega_0(1/4N)(2\pi mc/e\lambda_p B_p)^2$, where ω_0 is the pump-wave average beam waist along the interaction region. Table I summarizes some important parameters of a FEL operating at 4000 \AA using the scheme shown in Fig. 3. Also, for comparison, the characteristics of a similar system operating at a wavelength of 16 μm is included. It appears that the electron-beam requirements for laser operating at short wavelengths can be met using present electrostatic-accelerator technology. The Fermilab electron cooling experiment¹² expects to produce a continuous beam of 110-keV electrons ($I = 28 \text{ A}$). The expected electron-energy homogeneity and beam emittance from such a device is adequate to operate the FEL at 4000 \AA using the techniques discussed here.

The power losses used to calculate the efficiencies shown in Table I were completely dominated by copper-mirror losses in the pump-wave resonator. The mirror losses were estimated by extrapolating copper-mirror losses at 10.6 μm to the submillimeter and millimeter region using the classical theory of electrical conductivity of Drude. A factor-of-10 enhancement in reflectivity of copper mirrors can make this type of laser quite efficient ($e \sim 10\%$).

The author wishes to thank J. M. J. Madey, T. I. Smith, D. A. G. Deacon, J. N. Eckstein, and R. Taber for many useful discussions. This work was supported by the U. S. Office of Naval Research Contract No. N00014-79-C00403.

¹J. M. J. Madey, J. Appl. Phys. **42**, 1906 (1971).

²L. R. Elias *et al.*, Phys. Rev. Lett. **36**, 717 (1976).

³D. A. G. Deacon *et al.*, Phys. Rev. Lett. **38**, 897 (1977).

⁴L. R. Elias *et al.*, Stanford High Energy Physics Lab Report No. HEPL-812, 1976 (unpublished).

⁵A. Renieri, Comitato Nazionale per l'Energia Nucleare-Frascati Report No. 77-30, 1977 (unpublished); L. R. Elias *et al.*, Stanford High Energy Physics Lab Reports No. HEPL-824 and No. HEPL-831, 1978 (unpublished).

⁶J. M. J. Madey, Ph.D. thesis, Stanford University, 1970 (unpublished), p. 150; J. Bridges *et al.*, *Fermilab Electron Cooling Experiment Design Report* (U. S. GPO,

Washington, D. C., 1978).

⁷W. B. Colson, *Physics of Quantum Electronics* (Addison-Wesley, Reading, Mass., 1977), Vol. 5.

⁸W. H. Louisell *et al.*, Phys. Rev. A **18**, 655 (1978).

⁹H. Kildal and R. L. Byer, Stanford Microwave Report No. MW-83, 1970 (unpublished).

¹⁰R. H. Pantell *et al.*, IEEE J. Quantum Electron. **4**, 905 (1968).

¹¹N. M. Kroll and W. A. McMullin, Phys. Rev. A **17**, 300 (1978); F. A. Hopf *et al.*, Opt. Commun. **18**, 413 (1976).

¹²See Bridges *et al.*, Ref. 6.

“Convective” Loss-Cone Instability Is Absolute

M. J. Gerver

Laboratory of Plasma Studies, Cornell University, Ithaca, New York 14853

(Received 11 December 1978)

The high-frequency “convective” loss-cone mode in a mirror-confined plasma is shown to be absolutely unstable as a result of wave reflection from the mirror throats, provided that the plasma length is greater than an axial wavelength. Critical lengths for stability are only a few ion gyroradii for fusion parameters, much smaller than previous estimates. This result places serious limitations on the design of mirror fusion reactors, and precludes the possibility of a linearly stable reactor with empty loss cone.

The high-frequency convective loss-cone (HFCLC) mode was first considered in 1966 by Post and Rosenbluth,¹ who showed that it would seriously limit plasma confinement in a magnetic mirror machine more than a few hundred ion gyroradii in length, but that, in the absence of wave reflection at the mirror throats, it would not grow to significant levels in shorter machines. Since then, a number of possible reflection mechanisms have been considered. Aamodt and Book² pointed out that even if the wave has no turning points where $k_{\parallel}(z)=0$ (z being the axial coordinate and k_{\parallel} the axial wave number in the WKB approximation), there will still be a small amount of reflection, of order $\exp(-k_{\parallel}a)$, where a is the scale length of the mirror throats. This reflection can be interpreted as being due to the slight corrections to the WKB approximation. Equivalently it may be viewed as being due to reflection of the wave from complex turning points at which $k_{\parallel}(z)=0$, where $k_{\parallel}(z)$ has been extended analytically into the complex z plane. Since the wave grows by a factor of $\exp(-\text{Im}k_{\parallel}L)$ as it traverses the length of the machine ($\text{Im}k_{\parallel} < 0$ indicates growth), an absolute instability will occur if $|\text{Im}k_{\parallel}|L > k_{\parallel}a$. Aamodt and Book² considered those modes with the highest convective growth rates, viz. $\omega \simeq \omega_{p_i}$ and $k_{\perp}\lambda_D \simeq 1$, and for

these modes $|\text{Im}k_{\parallel}| \ll k_{\parallel}$; so absolute instability does not occur, although the critical length is somewhat reduced.

Other reflection mechanisms include nonlocal wave reflection due to coherent bouncing of electrons,³ and reflection from turning points due to ion cyclotron resonances.⁴ With any reflection mechanism, the axial wavelength is reduced by electromagnetic (finite β) effects,⁵ and this can reduce the critical length. Taking all of these effects into account, recent estimates⁶ of the critical length have been about 50 gyroradii, considerably less than the original estimate,¹ but still quite tolerable for a mirror fusion reactor.

In this Letter, I consider only the reflection mechanism discussed by Aamodt and Book.² When longer-wavelength modes ($k_{\perp}\lambda_D \ll 1$, $\omega \ll \omega_{p_i}$) are considered, then $\text{Im}k_{\parallel} \simeq k_{\parallel}$, and absolute instability occurs, even though the local convective growth rates are lower than for the modes considered by Aamodt and Book.² The critical length for these modes should be roughly one axial wavelength. For fusion parameters and for the worst modes, the critical length is only a few ion gyroradii. If the length of the mirror machine is less than a few ion gyroradii, then the radius of the plasma must also be less than a few ion gyroradii, and the plasma will be subject to the drift-